Hindawi
International Journal of Corrosion
Volume 2021, Article ID 6662395, 13 pages
https://doi.org/10.1155/2021/6662395

Research Article

Corrosion Inhibition of 3003 Aluminum Alloy in Molar Hydrochloric Acid Solution by Olive Oil Mill Liquid By-Product

M. Chadili,[1] M. M. Rguiti,[1] B. El Ibrahimi,[1] R. Oukhrib,[1] A. Jmiai,[1] M. Beelkhaouda,[2] L. Bammou,[2] M. Hilali,[1] and L. Bazzi[3]

[1]*Team of Physical Chemistry and Environment, Faculty of Sciences, University of Ibn Zohr, Agadir, Morocco*
[2]*Laboratory of Applied Chemistry and Environment, ENSA, University Ibn Zohr, PO Box 1136, Agadir, Morocco*
[3]*Industrial & Logistic Laboratory, Higher School of Management, Telecommunications and Computer Science, SUP MTI, Rabat, Morocco*

Correspondence should be addressed to B. El Ibrahimi; brahim.elibrahimi@edu.uiz.ac.ma

Received 5 October 2020; Revised 4 January 2021; Accepted 12 January 2021; Published 28 January 2021

Academic Editor: Michael I. Ojovan

According to the literature, the works on the inhibition of aluminum alloy corrosion using naturally occurring compounds are limited. For this, the inhibiting effect of oil mill liquid by-product (OMW) on the corrosion of 3003 aluminum alloy (AA3003) in molar hydrochloric acid solution was evaluated using electrochemical techniques. In parallel, a computational approach based on DFT/B3LYP and *Monte Carlo* methods was used to understand the inhibition process under electronic and atomic scales, respectively. The experimental results reveal that OMW has a good inhibiting effect on the corrosion of AA3003 alloy in the tested solution and acts as a cathodic inhibitor. The inhibitory efficiency increases by increasing OMW concentration to attain 89% at 6.0 ppm. The effect of temperature shows that the inhibition efficiency of OMW decreases with temperature rising. Nevertheless, a good prevention capacity of 83% is obtained at 338 K. Such interesting achieved protection property was attributed to the adsorption of OMW constituents onto the alloy surface via a mixed physichemisorption process. This process is found to obey the Langmuir adsorption isotherm. Furthermore, the activation thermodynamic parameters of the corrosion process of AA3003 alloy were also determined and discussed. The computational outcomes outlined the ability of the OMW components to interact favorably with the metal surface, hence the formation of a protective layer, which justified the observed inhibition behaviors. Conferring to the present study, OMW can be used as a good green corrosion inhibitor for AA3003 alloy in the acidic medium.

1. Introduction

The corrosion affects the industrial sector and can cost billions of dollars each year [1]. Besides, it causes a significant loss of energy and contributes to environmental degradation [2]. In the case of industrial processes, metals and metal alloys are attacked by acid solutions, which act as aggressive agents. In general, acids are heavily used in industry, mainly in industrial cleaning, petroleum refining, and petrochemical processes [3, 4]. Aluminum and its alloys are widely used in various fields because of their physicochemical properties compared to other materials [5]. The corrosive medium of hydrochloric acid is commonly used for chemical or electrochemical cleaning and acid stripping of aluminum. In aqueous solutions, a passive oxide film will be formed which is compact and adheres to the aluminum surface [6]. The film (amphoteric) formed is substantially dissolved in an acidic or basic medium and undergoes the corrosion phenomena [7, 8]. To combat this scourge, several techniques are used: alloy selection, anodic protection, and the use of inhibitors [9, 10]. The introduction of corrosion inhibitors into the aggressive solution is an effective method to stop or delay corrosion by using organic or inorganic compounds [11, 12].

Until now, organic compounds containing N, O, P, or S heteroatoms are considered to be good corrosion inhibitors for aluminum in the acid environment, especially aromatic amines [13], carbonyl compounds [14], amino acids [15], phenols [16], polymers [17], and aliphatic amines [18, 19].

However, among those compounds, they have high toxicity to humans and the environment [20–22]. In recent decades, various studies have focused on the use of so-called ecological or green herbal inhibitors, namely, extracts and essential oils of aromatic and medicinal plants [23]. The choice of these ecological inhibitors essentially resides in their cost, their biodegradability, and a high efficiency generally exceeding 95% at low concentrations [23–26]. On the other hand, they are known as reducers of the corrosion of metals and their alloys in the acidic environment, to replace the toxic products currently used [27]. The inhibitory effect of these green inhibitors is due to the presence of high variability and richness of organic compounds that can be adsorbed on the metal surface, which leads to the formation of a protective film and therefore causes the limitation of the corrosion phenomenon [28, 29].

Each year, several industrial processes in the Mediterranean region, such as Morocco, release large quantities of liquid waste during the olive oil production season [29]. These effluents, so-called olive oil mill wastewaters (OMW), can be considered a source of ecological inhibitors. OMW contains a variety of phenolic compounds with heterocyclic structures comprising nitrogen and oxygen atoms, which are responsible for inhibiting the corrosion process [30]. Furthermore, these effluents are not too expensive from an economic point of view compared to conventional synthetic inhibitors. Several authors have evaluated the property of OMW to act as a corrosion inhibitor. They have found better corrosion inhibition performances for steel [31] and iron [32]. In this regard, exploiting OMW as a corrosion inhibitor on an industrial scale can minimize also the damage to the environment. According to the available literature, there is no work yet on the use of OMW as anticorrosion compounds for aluminum alloys. For this, the current study will be focused on this subject.

According to the above-mentioned view, this work is aimed at examining the protective effect of OMW toward the corrosion of 3003 aluminum alloy in 1 M hydrochloric acid. To evaluate the protective power of this inhibitor, potentiodynamic polarization and electrochemical impedance spectroscopy techniques were used. In this regard, the influence of OMW concentration and temperature on the observed inhibition behaviors was investigated.

In recent years, the computational demarche has been widely served to investigate the inhibition process of metallic corrosion at electronic and atomic scales by using DFT and Monte Carlo methods, respectively [31, 32]. Besides, it is recognized that OMW is a mixture of several phenolic-based compounds [33]. In the present study, we have limited our electronic and atomic inspections on tyrosol L (Tyr) and hydrotyrosol L (HydroTyr) molecules, which are its major constituents [34]. In this context, we limited the use of the DFT/B3LYP method to investigate the reactivity of Tyr and HydroTyr molecule and their implicit interfacial interaction with the aluminum surface as well [31, 35], while the explicit interactions were discussed using the Monte Carlo/simulated annealing method as reported widely in the literature [36].

2. Materials and Methods

2.1. Materials and Solutions. All used reagents in this work were analar grade, and the distilled water was used to prepare solutions. The used aggressive solution (1 M HCl) was prepared by diluting a commercial hydrochloric acid solution (37%), provided by Fuka, with distilled water. A 3003 aluminum alloy (AA3003 notation will use subsequent) plate was used to conduct the current study. The composition of AA3003 alloy is summarized in Table 1.

The OMW samples used in this study were taken from the third phase olive mill located in the region of Essaouira, Morocco (Mejji olive mill). The sample of OMW has been obtained from olives well-ripened and stored at 4°C. The effluent was subjected to several successive filtrations to remove the maximum suspended matter. The physicochemical characterizations of OMW were carried out according to the standard analytical methods for the examination of water and wastewater [37, 38]. The physicochemical characteristics of OMW are listed in Table 2.

In order to study the inhibition capacity of OMW against the corrosion of AA3003, 10 mL of OMW is added to one liter of 1 M HCl solution, which is stirred for 30 min. The resulting aqueous solution was stored as the stock solution in the dark and at 4°C [39]. OMW concentrations ranging from 0.5 to 6.0 ppm were prepared by diluting the stock solution using 1 M HCl solution.

2.2. Electrochemical Methods. The AA3003 plate was used to prepare the working electrode for the electrochemical study, which was cut to obtain a rod and then mounted in glass tubes with a two-component epoxy resin leaving a contact area of 0.16 cm^2. For the electrochemical tests, we used a thermostatic triple-walled glass cell with a platinum counter-electrode and a saturated calomel reference electrode. Prior to each experiment, the surface of the working electrode was mechanically polished using 1200-grade emery paper, washed with distilled water, and rapidly transferred to the electrochemical cell containing the test solution.

The electrochemical measurements were performed using a VersaStat3 potentiostat/galvanostat and VersaStudio as control software. Prior to each experiment, the open circuit potential (OCP) of the AA3003 working electrode was measured as a function of time for 30 min, which was the appropriate time to reach a quasistationary state. The electrochemical impedance spectra have been recorded at the steady OCP value with 10 mV as the amplitude of the superimposed alternating signal, and the applied frequency varied from 100 kHz to 0.01 Hz. The anodic and cathodic polarization experiments were carried out at a scanning rate of 1 mV s^{-1} between -1200 and -500 mV/SCE. To achieve reproducibility, each experiment was repeated at least three times. The EIS data is analyzed with software based on a simplex regression of the parameters (ZSimpWin 3.1 software). All experiments were performed in a stagnant natural aerated solution at the chosen temperature using a water thermostat.

2.3. DFT Calculations. The electronic structure of the two main constituents of OMW (i.e., Tyr and HydroTyr) was

Table 1: Nominal composition of used AA3003 alloy.

Element	Fe	Si	Cu	Zn	Mn	Ni	Ti	Mg	Cr	Al
Content (%)	0.19	0.44	<0.03	<0.002	0.04	<0.003	<0.002	0.53	<0.002	Balance

Table 2: Physicochemical characterization of EOMW used in the corrosion tests.

Parameter (unit)	Value
Turbidity (NTU)	2805
pH	5.22
Conductivity (ms cm^{-1})	10.52
BOD_5 (g L^{-1})	62
COD (g L^{-1})	180
K (g L^{-1})	2.91
Na (g L^{-1})	2.71
Cl (g L^{-1})	3.37
Density (g mL^{-1})	1.03

studied using the DFT/B3LYP/6-311G(d,p) level of theory as implemented in Gaussian (version 09) software [40]. The aqueous phase was treated using the IEFPCM solvation model and setting water as solvent [41]. After the geometry optimization stage, some relevant electronic descriptors, i.e., gap energy (ΔE), chemical hardness (η), fraction of electrons transferred (ΔN), and total negative charge (TNC), of the molecules were calculated. The latest descriptors have been fully defined elsewhere, e.g., see [42]. To investigate the favorable centers of adsorption within these molecules, the frontier molecular orbital repartitions and the molecular electrostatic potential (ESP) map were plotted using Gauss-View (version 05) software and then discussed [43].

2.4. Monte Carlo Simulations. To investigate the adsorption process of Tyr and HydroTyr on the aluminum surface, the Monte Carlo simulations were carried out in the aqueous phase (100 H_2O). The metallic substrate was modeled by five layers of Al(111) surface with 17.2 Å ×17.2 Å dimensions [44]. To avoid the possible intersupercell interactions that can be caused by the periodic boundary condition, a sufficient vacuum region of 50 Å is used [45]. Van der Waals and electrostatic interactions were treated using atom-based and Ewald summation methods, respectively. As a force field, the COMPASS is employed [46]. For the simulated annealing process, ten cycles of heat are used with 100 000 steps per each cycle. To get accurate results, the smart algorithm is employed and the convergence tolerances were fixed at 2×10^{-5} kcal mol^{-1}, 10^{-3} kcal mol^{-1} $Å^{-1}$, and 10^{-5} Å for energy, force, and displacement, respectively. The simulations were carried out using Material studio (version 06) software.

3. Results and Discussion

3.1. Potentiodynamic Polarization Results. The effect of the concentration of OMW on the corrosion behavior of AA3003 alloy in the 1 M HCl solution was studied by using

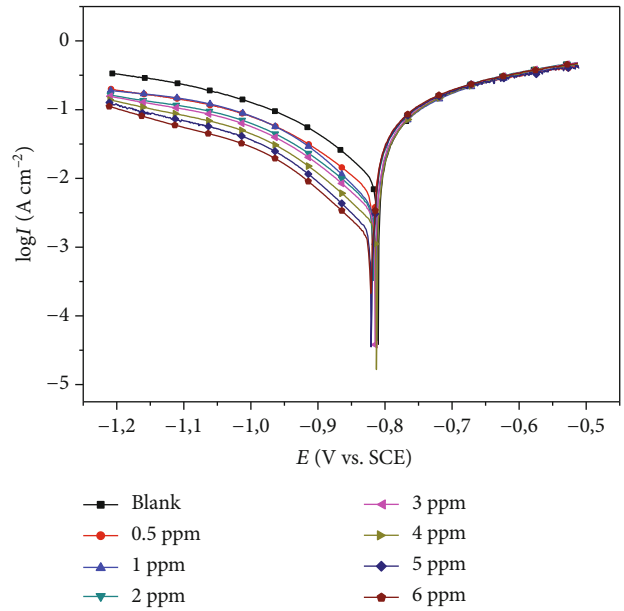

Figure 1: Polarization curves of AA3003 alloy in 1 M HCl solution without and with addition of OMW at different concentrations (at 298 K).

anodic and cathodic polarization measurements after 30 min of the immersion time. Figure 1 illustrates the potentiodynamic polarization curves for the alloy understudy in the absence and presence of OMW with different concentrations at 298 K.

As can be seen in the anodic branch (Figure 1), we can point out the difficulty of recognizing the linear region of the Tafel law. Hence, the current densities are determined by extrapolating only the Tafel cathodic linear region to the corrosion potential. This method of adjustment was used by several authors for aluminum-based materials in the hydrochloric acid medium [25, 47]. The relevant determined electrochemical parameters, namely, current density (I_{corr}), corrosion potential (E_{corr}), and cathodic slope (β_c), as well as the inhibitory efficiency (IE (%), Equation (1)) as a function of the OMW concentration, are tabulated in Table 3:

$$\text{IE}(\%) = \left(1 - \frac{I'_{corr}}{I_{corr}}\right) \times 100, \quad (1)$$

where I_{corr} and I'_{corr} are, respectively, the uninhibited and inhibited corrosion current densities of AA3003 alloy.

It is clear from Table 3 that the Tafel cathodic slope (β_c) changes slightly in the presence of the OMW, which outlines no significant effect of OMW on the hydrogen reduction mechanism. Such a conclusion can be revealed from Figure 1 from which the cathodic polarization curves are

Table 3: Derived polarization electrochemical parameters of AA3003 alloy in 1 M HCl medium in the absence and presence of OMW at different concentrations (at 298 K).

Conc. (ppm)	I_{cor} (mA cm^{-2})	$-E_{cor}$ (mV/SCE)	$-\beta_c$ (mV/dec)	IE (%)	θ
Blank	11.866	811	134	—	—
0.5	7.619	822	143	35.79	0.3579
1.0	5.140	812	131	56.68	0.5668
2.0	4.403	819	125	62.89	0.6289
3.0	4.090	812	136	73.94	0.7394
4.0	2.127	815	132	82.07	0.8207
5.0	1.894	819	138	84.00	0.8400
6.0	1.419	816	115	88.04	0.8804

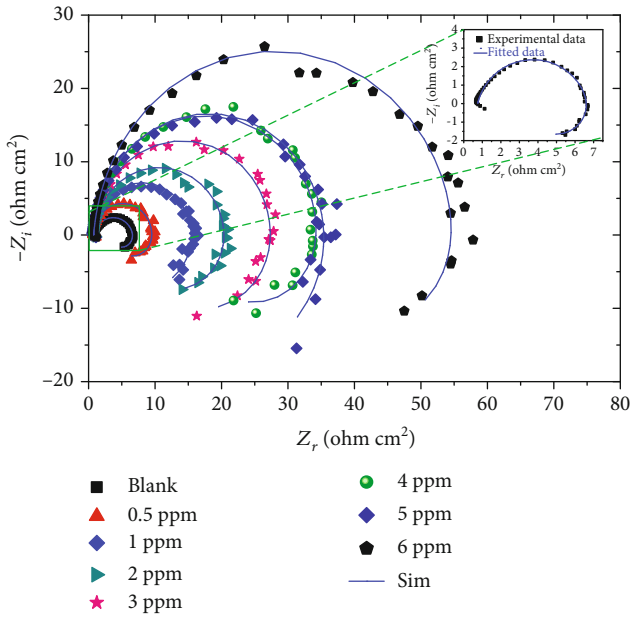

Figure 2: Nyquist plots of AA3003 alloy in 1 M HCl solution without and with addition of OMW at different concentrations (at 298 K).

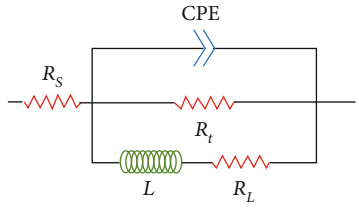

Figure 3: Equivalent electrical circuit used to model the experimental impedance data illustrated.

almost parallel. On the other hand, it is found that the value of I_{corr} decreases with the addition of the OMW, which induces an increase of the inhibition efficiency as a function of the OMW concentration. This is due to the increase of the blocked fraction of the alloy surface by the adsorption of the active components present in OMW, as well as their synergistic effect [48]. The prevention effectiveness reaches 88% with a low concentration of OMW (6.0 ppm), indicating that OMW is an excellent inhibitor of AA3003 alloy in the 1 M HCl medium. Conferring to Figure 1, the OMW can be classified as a cathodic inhibitor due to the reduction of cathodic currents by its addition with respect to the uninhibited solution [49].

Table 4: Mathematical expression of evaluated adsorption isotherms and its corresponding calculated R^2 values.

Adsorption isotherm	Equation	R^2
Flory-Huggins	$\ln\left(\frac{\theta}{C}\right) = \ln(K_{ads}) + x\ln(1-\theta)$	0.92
Freundlich	$\ln\theta = \ln(K_{ads}) + n\ln C$	0.94
El-Awady	$\ln\left(\frac{\theta}{1-\theta}\right) = \ln(K_{ads}) + \gamma\ln C$	0.96
Temkin	$\theta = -\frac{1}{2a}\ln(K_{ads}) - \frac{1}{2a}\ln C$	0.97
Frumkin	$\ln\left[C\times\frac{\theta}{1-\theta}\right] = \ln(K_{ads}) + 2\alpha\theta$	0.98
Langmuir	$\frac{C}{\theta} = \frac{1}{K_{ads}} + C$	0.99

3.2. Electrochemical Impedance Spectroscopy Results. The Nyquist diagrams for studied aluminum alloy in 1 M HCl medium at 298 K, in the absence and presence of different OMW concentrations, were plotted in E_{OCP} potential after 30 min of immersion as depicted in Figure 2. It is evident from this figure that the impedance diagrams consist of a large capacitive loop at high frequency followed by an inductive loop at low frequency. The first loop is due to the formation of an oxide film on the aluminum surface, while the second one is attributed to the relaxation of the charged intermediates adsorbed on the surface tested [50, 51]. In addition, the inductive semicircle diameter is considerably less than that observed in high frequencies. On the other hand, the impedance spectrum shows an approximately elliptical shape that is attributed to the frequency dispersion due to the roughness and inhomogeneity of the metal surface

Table 5: Electrochemical impedance parameters of AA3003 alloy in 1 M HCl medium without and with addition of OMW inhibitor at different concentrations (at 298 K).

Conc. (ppm)	χ^2	$R_S(\Omega\,\mathrm{cm}^2)$	$R_t(\Omega\,\mathrm{cm}^2)$	$R_L(\Omega\,\mathrm{cm}^2)$	$Q(\mathrm{S\,s}^n\,\mathrm{cm}^{-2})$	n	$\mathrm{L(H\,cm}^2)$	IE (%)	θ
Blank	1.73×10^{-2}	0.75	5.95	4.58	333	0.8573	1.613	—	
0.5	1.85×10^{-2}	0.74	8.78	4.64	90.8	0.9897	2.019	32.2	0.322
1.0	1.90×10^{-2}	0.73	14.74	5.64	61.7	0.9847	4.776	59.6	0.596
2.0	1.81×10^{-2}	0.73	19.77	6.50	94.4	0.9882	5.074	69.9	0.699
3.0	1.98×10^{-2}	0.71	26.85	8.66	123.0	0.9787	6.822	77.8	0.778
4.0	2.03×10^{-2}	0.72	30.72	8.27	72.6	0.9557	11.15	80.6	0.806
5.0	2.13×10^{-2}	0.72	34.78	43.68	62.6	0.9680	14.71	82.9	0.829
6.0	1.63×10^{-2}	0.77	54.42	61.97	84.0	0.9486	38.06	89.1	0.891

[48]. In the acidic media, similar impedance spectra have been reported in the corrosion literature for aluminum and its alloys [23, 25, 26, 28–30, 49–64]. The addition of the OMW does not affect the shape of the loops, indicating that no change in the corrosion mechanism of AA3003 alloy has occurred [65]. The impedance data are simulated by using the equivalent circuit illustrated in Figure 3 [66]. The components of this circuit are the electrolyte resistance (R_s), charge transfer resistance (R_t), and constant phase element (CPE) for the used electrode, and L and R_L represent the inductance and the inductive resistance associated with the inductive loop, respectively. Accordingly, the calculated impedance parameters are given in Table 4. The inhibitory efficiency derived from the charge transfer resistance is obtained by the following relationship [49, 58, 65]:

$$\mathrm{IE}\,(\%) = \left(1 - \frac{R_t^0}{R_t}\right) \times 100, \tag{2}$$

where R_t^0 and R_t are the charge transfer resistances of AA3003 alloy without and with the OMW inhibitor, respectively.

As can be noted in Figure 2 and from the values of χ^2 in Table 5, a good fit by using the chosen equivalent circuit was obtained. This means that the adjusted data have good agreement with the experimental data. According to Table 5, the R_t values increase with increasing OMW concentration, resulting in an increase in IE(%) attributed to the increase in organic inhibitory molecules (i.e., polyphenols) adsorbed on the surface of aluminum alloy [26, 58]. IE(%) attains a maximum value equal to 89%, which confirms that OMW has a good protection ability for AA3003 alloy in 1 M HCl medium. The IE(%) values computed from the EIS measurements are in good agreement with those found by the potentiodynamic technique [67]. Besides, conferring to the obtained Q values in the presence of the tested inhibitor, it can be assumed that the OMW active constituents were adsorbed onto the alloy surface to form a protective layer [68].

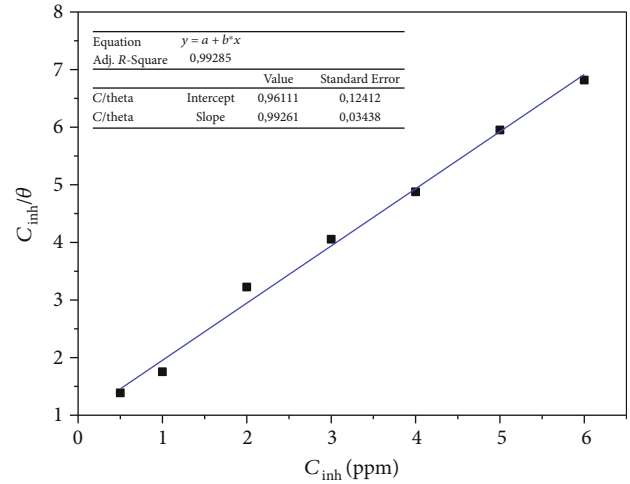

Figure 4: Langmuir isotherm line of AA3003 alloy in 1 M HCl medium with different concentrations of OMW at 298 K.

3.3. Adsorption Isotherm. The adsorption process depends on several electronic properties of the inhibitor tested, the nature of the metal surface, the temperature, etc. [69]. The purpose of the use of adsorption isotherms is to describe the mechanism of interaction between the metal surface and the inhibitor (i.e., OMW). To understand the type of adsorption of OMW on the surface of the aluminum alloy in the 1 M HCl solution, it is important to study the relationship between the inhibitory power and the surface coverage (θ, Equation (3)) for different concentrations of OMW. Different adsorption isotherms were evaluated to find the best fit for the experimental data driven from potentiodynamic polarization technique. Table 4 summarizes the linear determination coefficients (R^2) with equation expressions for each examined isotherm, namely, Langmuir, Freundlich, Temkin, Frumkin, Flory Hoggins, and El-Awady [55, 70–72]. According to the obtained R^2 values, it is apparent that the adsorption of the OMW inhibitor on the surface of the alloy favorably obeys the Langmuir adsorption isotherm (Figure 4) [60]. In the equation of this isotherm, C is the

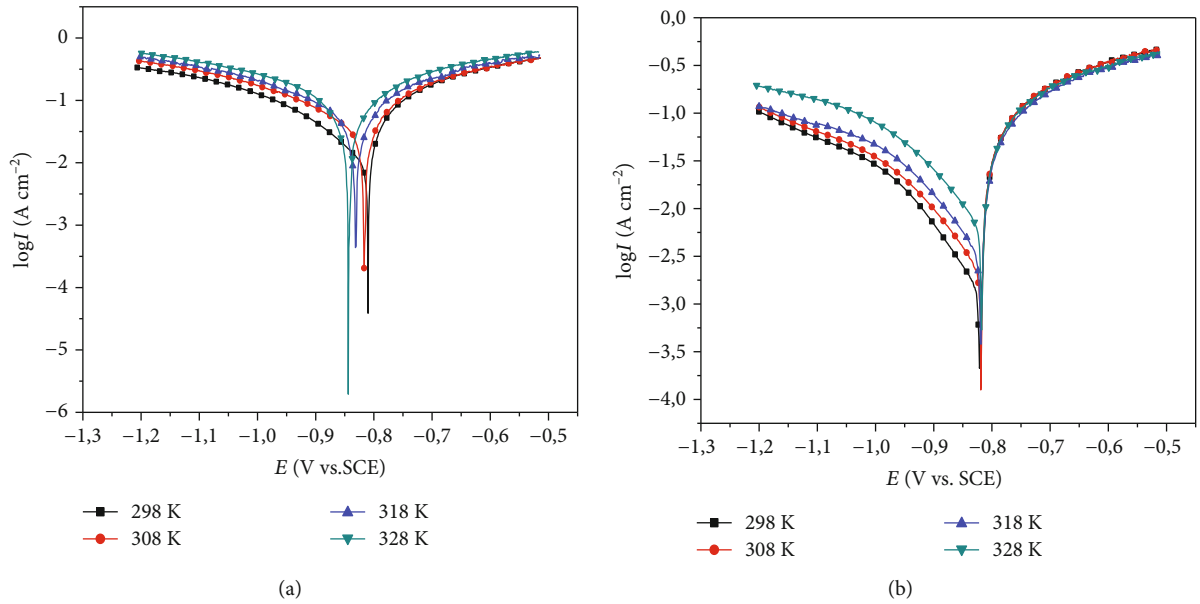

Figure 5: Polarization curves of AA3003 alloy in 1 M HCl medium (a) without and (b) with addition of 6.0 ppm OMW at different temperatures.

Table 6: Derived polarization electrochemical parameters of AA3003 alloy in 1 M HCl medium in the absence and presence of 6.0 ppm OMW at different temperatures.

	T (K)	I_{corr} (mA cm^{-2})	$-E_{corr}$ (mV/SCE)	$-b_c$ (mV/dec)	IE (%)	θ
Blank	298	11.866	811	134	—	—
	308	24.790	817	151	—	—
	318	37.067	829	153	—	—
	328	41.559	841	156	—	—
6.0 ppm	298	1.419	822	115	88.04	0.8804
	308	3.162	824	124	87.56	0.8756
	318	5.011	817	121	87.30	0.8730
	328	7.135	818	143	83.14	0.8314

OMW concentration and K_{ads} represents the adsorption equilibrium constant:

$$\theta = 1 - \frac{I'_{corr}}{I_{corr}}. \quad (3)$$

To explain the nature of the interaction between the AA3003 surface and the adsorbed OMW molecules, the thermodynamic adsorption energy, ΔG^0_{ads} (Gibbs free energy), was determined using the following relationship [49, 73]:

$$\Delta G^0_{ads} = -RT \ln \left(1 \times 10^6 K_{ads}\right), \quad (4)$$

where R denotes the universal gas constant (8.314 J mol^{-1} K^{-1}), T is the absolute temperature (K), and 1×10^6 value is the concentration of water (C_{H_2O}) calculated in mg L^{-1}.

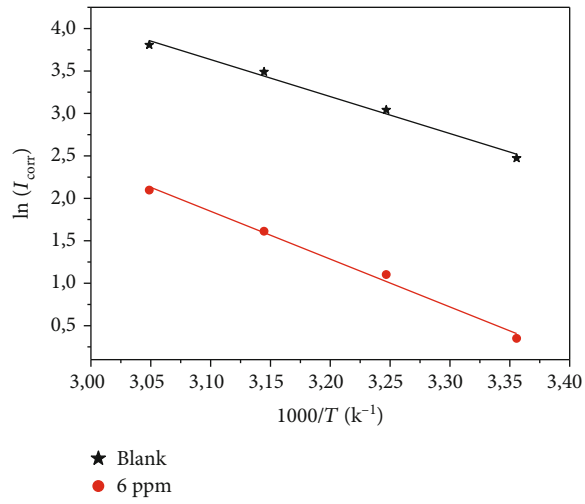

Figure 6: Arrhenius plots of AA3003 alloy in 1 M HCl in the absence (black line) and presence (red line) of OMW at 6.0 ppm.

The calculation of the value of ΔG^0_{ads} at 298 K gives –34.32 kJ mol^{-1}. This negative value indicates that the adsorption of the inhibitor is spontaneous [74], and the interaction of adsorbed OMW molecules on the AA3003 surface is strong [49]. Depending on the value of ΔG^0_{ads}, one can distinguish the type of adsorption of an inhibitor onto the metal surface. According to Chu and Sukava and Sangeetha et al. [75, 76], the energy values (ΔG^0_{ads}) up to -20 kJ mol^{-1} indicate the presence of electrostatic interactions (physisorption) between the metal surface and the inhibitor. While if the values of ΔG^0_{ads} are lower than -40 kJ mol^{-1}, the inhibitory molecules form more stable chemical bonds with the material (chemical adsorption). In our study, the calculated value of ΔG^0_{ads} (-34.32 kJ mol^{-1}) outlines that the adsorption mechanism of OMW molecules onto the AA3003 surface is a mixed type, i.e., involves both physical and chemical adsorption processes [76].

3.4. Effect of Temperature. Temperature is one of the parameters that affect the corrosion phenomenon of metallic materials. The aim to study the effect of temperature is to examine the stability of the tested inhibitor. The influence of temperature on the corrosion of AA3003 in 1 M HCl solution in the absence and presence of 6.0 ppm OMW was performed in the temperature range of 298 to 328 K. Under these conditions, Figure 5 illustrates the obtained polarization curves, and their corresponding extracted parameters are summarized in Table 6.

From the obtained results, it can be revealed that the increase in temperature has no significant effect on the shape of the polarization curves (Figure 5), hence the mechanism of AA3003 alloy corrosion. In addition, the values of current densities (I_{corr}) in the presence and absence of OMW increase clearly with increasing temperature (Table 6). In these circumstances, the inhibitory efficiency decreases with the rise in temperature of the electrolytic medium. According to several authors, the latter behavior is due essentially to the desorption of inhibitor molecules, which is to say, the reduction of the inhibitor capacity to be adsorbed on the metallic surface at the elevated temperatures [55, 77–79].

In order to explain the adsorption mechanism of an inhibitor, it is necessary to determine some thermodynamic parameters of activation for the studied system, namely, E_a, ΔH^*, and ΔS^*). Figure 6 shows the variation of the logarithm of the corrosion current density (ln I_{corr}) of AA3003 as a function of (1000/T) in 1 M HCl solution in the absence and presence of OMW at 6.0 ppm. The found correlation coefficients for the obtained straight lines are 0.9. The slopes of these lines are used to determine the activation energies (E_a) according to the Arrhenius equation:

$$I_{corr} = A \exp\left(-\frac{E_a}{RT}\right), \quad (5)$$

where T denotes the absolute temperature (K), R is the universal gas constant (J mol^{-1} K^{-1}), and A is the Arrhenius constant.

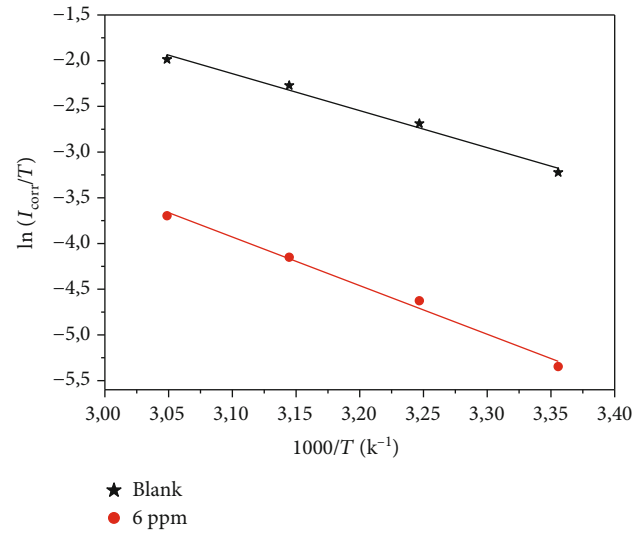

Figure 7: Arrhenius transition state plots of ln(I_{corr}/T) as a function of 1000/T for the systems under study.

Table 7: Determined activation energies for AA3003 corrosion in 1 M HCl medium without and with OMW inhibitor at 6.0 ppm.

Medium	E_a (kJ mol^{-1})	ΔH^* (kJ mol^{-1})	ΔS^* (J mol^{-1} K^{-1})
Blank	36.24	33.64	-111.04
+6.0 ppm of OMW	46.82	44.22	-93.11

Table 8: Some relevant electronic structure parameters of Tyr and HydroTyr molecules.

Molecule	ΔE (eV)	η (eV)	TNC (e)	ΔN (e)
Tyr	6.396	3.198	-2.011	0.146
HydroTyr	5.612	2.806	-1.970	0.251

The activation energies (i.e., ΔH^* and ΔS^*) are determined using the following Arrhenius transition state equation:

$$I_{corr} = \frac{RT}{Nh} \exp\left(\frac{\Delta S^*}{R}\right) \exp\left(-\frac{\Delta H^*}{RT}\right), \quad (6)$$

where N represents the Avogadro number ($N = 6.02252 \times 10^{23}$ mol^{-1}), h is the Planck constant ($h = 6.626176 \times 10^{-23}$ J s), and ΔS^* (entropy) and ΔH^* (enthalpy) are the activation parameters. Figure 7 demonstrates the shape of ln (I_{corr}/T) as a function of 1000/T for the systems under study. Straight lines are obtained with an equal slope ($-\Delta H^*/R$) and extrapolation of lines (ln $R/Nh + \Delta S^*/R$) [68]. The values of E_a, ΔH^*, and ΔS^* are listed in Table 7 for AA3003 in 1 M HCl medium without and with OMW inhibitor at 6.0 ppm.

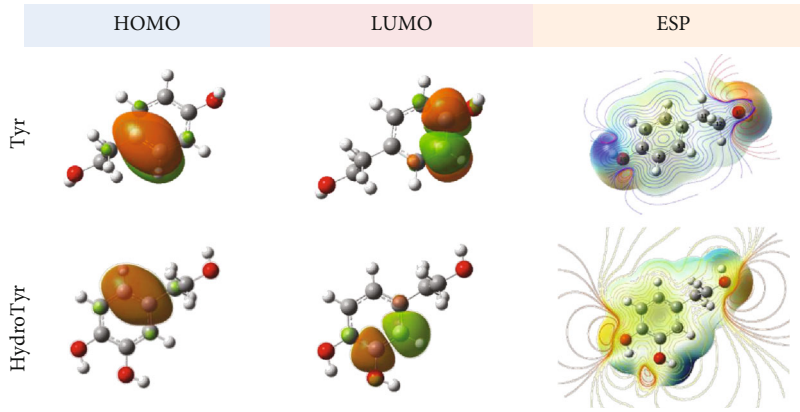

Figure 8: Isosurface of frontier molecular orbitals (i.e., HOMO and LUMO) and ESP map (red (blue) color refers to negative (positive) potential) of Tyr and HydroTyr molecules.

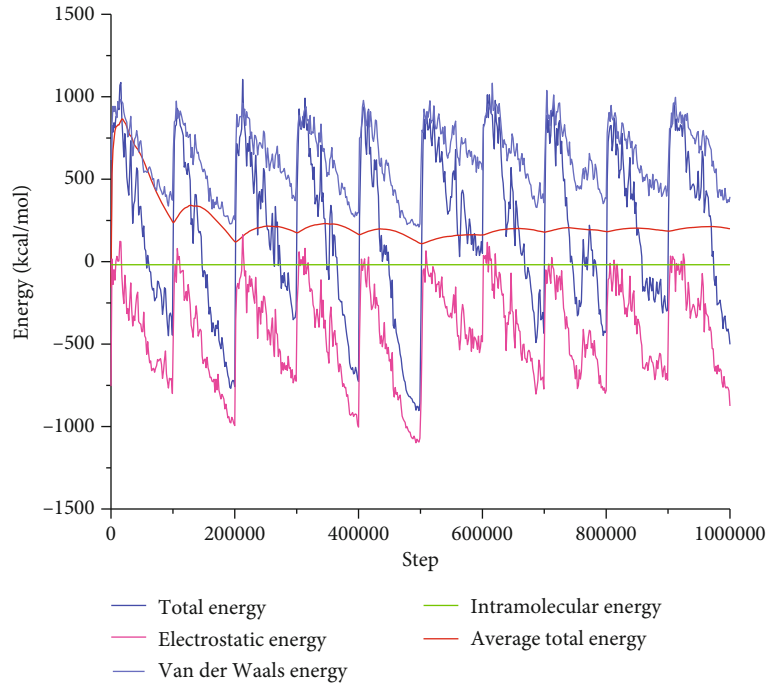

Figure 9: Energetic profile of HydroTyr molecule during the Monte Carlo simulation under explicit solvation condition.

According to the obtained data, the calculated activation energy (E_a) values for the uninhibited solution without and with OMW are 36.24 and 46.82 kJ mol^{-1}, respectively. It is noted that the activation energy increases in the presence of OMW, which indicates that the AA3003 alloy corrosion process has been modified; this may be attributed to the influence of the molecules existing in OMW on this interfacial process [6]. Moreover, the tabulated values of ΔH^* are positives that reflect the endothermic nature of the AA3003 dissolution process. It is evident that the activation energy increases sharply in the presence of the inhibitor. This is due to the adsorption of the inhibitory species on the surface of the alloy [71, 72, 80]. Besides, the entropy ΔS^* increases more positively with the presence of the OMW inhibitor, in which the obtained values are -111.04 and -93.11 J mol^{-1} K^{-1} for the 1 M HCl medium without and with the addition of the inhibitor, respectively. These results imply the formation of a stable and ordered layer of this inhibitor on the AA3003 surface [81], and the negative sign of ΔS^* indicates that the activated complex represents an association rather than a step of dissociation, which means that a decrease in the disorder occurs by passing reagents to the activated complex [6, 82].

3.5. DFT Results. The relevant electronic structure parameters of Tyr and HydroTyr molecules in the aqueous phase are summarized in Table 8. Agreeing with Fukui's theory, the molecule reactivity depends on its frontier molecular orbitals [83]. Under this concept, the energy gap (ΔE) was largely used to expect the reactivity of numerous inhibitor molecules. According to many reports, the value of ΔE has been correlated with the observed inhibition efficiency, in which the decrease of ΔE leads to good corrosion prevention.

The calculated value of ΔE proposes that the HydroTyr molecule is more reactive than the Tyr one. Subsequently, the interaction of HydroTyr with the aluminum surface is more chemical than that of Tyr. On the other hand, the HydroTyr molecule can provide an enhanced prevention capacity as compared to Tyr.

The chemical reactivity can be further expected via the chemical hardness (η), which describes the polarization or the deformation abilities of the molecule [84]. In other words, the molecule with lower hardness easily tends to react and adsorb onto the metal surface, which results in its higher inhibition efficiency [85]. In our case, the lowest η value is obtained for HydroTyr as compared to Tyr. Therefore, we can conclude that HydroTyr interacts more effectively with the aluminum surface; thus, it can provide the highest prevention efficiency.

It is well known that almost all metal surfaces are charged positively in the acidic media such as aluminum in our case. Consequently, the electrostatic interactions between the inhibitor molecules and metal surface will be great as the total negative charge (TNC) of thses molecules increased [86]. In the current study, the Tyr molecule displays more TNC negative value indicating its supplement tendency to interact electrostatically with aluminum surface regarding HydroTyr.

To elucidate the implicit interfacial interactions between the considered molecules and the aluminum surface, the fraction of transferred electrons (ΔN) was calculated using the work function of Al(111) face [87]. According to the tabulated values (Table 8), both molecules exhibit the tendency to denote electrons to the aluminum surface, which is higher for the HydroTyr molecule (0.251) as compared to Tyr (0.146). This finding outlines the affinity of HydroTyr to form chemical bonds with the metal surface than Tyr.

To explore the promising sites of adsorption within the Tyr and HydroTyr molecular skeleton, the distribution of frontier molecular orbitals and molecular ESP maps were plotted. Figure 8 displays the obtained molecular plots. As can be seen from this figure, both frontier molecular orbital densities are vastly located on the carbon atoms within the benzene ring, while small densities are placed in some extra-benzene ring atoms. These observations underline the role of the benzene moiety in the chemical process during the inhibitor/aluminum interfacial interactions, especially for the HydroTyr molecule [88]. On the other hand, as shown in Figure 8, the electron-rich regions characterized by negative potentials (i.e., red regions) are mainly located on the alcohol functions for both considered molecules. The intense negative potential can be noted in the Tyr molecule as compared to the HydroTyr one. This indicates the ability of these major OMW-containing molecules to interact electrostatically with electropositive sites upon aluminum through these extrabenzene functions [89].

3.6. Monte Carlo Simulations. In order to study, in detail, the adsorption process of the two chosen OMW constituents (i.e., Tyr and HydroTyr) on the aluminum surface, Monte Carlo simulations associated with the simulated annealing algorithm were carried out. Figure 9 illustrates the energetic profile of a considered OMW molecule (i.e., HydroTyr) during the simulation in the aqueous phase.

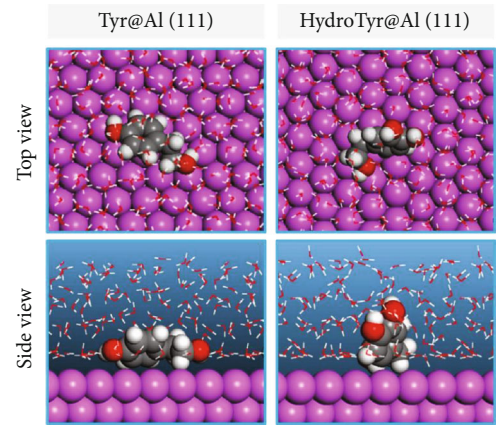

Figure 10: Top and side views of the equilibrium adsorption mode of Tyr and HydroTyr molecules onto Al(111) surface.

Figure 10 represents the most stable adsorption configuration of the selected OMW components on the Al(111) surface. According to the obtained configurations, it is clear that Tyr and HydroTyr are nearly placed on the metal surface. This outlines the affinity of these compounds to be adsorbed onto the aluminum surface, subsequently the formation of a protective layer that covers the metal surface [90]. The energetic aspect of the adsorption process shows that the binding energies are 66.847 and 68.004 kcal mol^{-1} for HydroTyr and Tyr, respectively. These values reflect the capacity of the considered OMW components to interact spontaneously and effectively with the Al(111) surface [91]. Furthermore, the observed energy ranking, i.e., HydroTyr < Tyr, indicates the enhanced ability of Tyr to adsorb on the metal surface through nonbonding interactions (i.e., electrostatic and Van de Waals interactions) [92]. On the other hand, it was found that the binding energy of water molecules is about 15 kcal mol^{-1}, which is lower than the corresponding ones of Tyr and HydroTyr molecules. Such finding underlines the affinity of OMW components to replace preadsorbed water molecules on the aluminum surface, which leads to the formation of a protective layer upon the metal surface [93, 94].

Given the above-mentioned statements, HydroTyr shows more tendency to interact with the aluminum surface through a chemical process rather than a physical (nonbonding interactions) one, whereas the opposite behaviors can be outlined for the Tyr molecule. Such finding explains the experimentally obtained value of ΔG^0_{ads} (-34.32 kJ mol^{-1}), which indicates the mixed physicochemical character of the adsorption process of OMW components onto the metal surface.

4. Conclusion

The effect of OMW on the corrosion behavior of AA3003 alloy in molar hydrochloride solution was investigated through electrochemical measurements complemented by thermodynamic studies and theoretical calculations. Based

on the obtained results, OMW acts as a good corrosion inhibitor for AA3003 alloy at lower concentrations with interesting protection efficiencies even at elevated temperatures. According to the thermodynamic parameters, the adsorption process of OMW constituents onto the alloy surface is a mixed physichemisorption type. On the other hand, computational simulations outlined the affinity of the major OMW components to interact with the aluminum surface, which leads to the formation of a protective layer. OMW can be used instead of conventional toxic compounds to prevent acidic corrosion of AA3003 alloy.

Data Availability

No data were used to support this study.

Additional Points

Highlights. (1) OMW has a good inhibiting effect (89%) on the corrosion of AA3003 alloy in 1 M HCl. (2) Good prevention capacities are obtained even at elevated temperatures. (3) DFT/B3LYP and *Monte Carlo* methods were used to understand the inhibition process. (4) Major OMW components interact favorably with the metal surface.

Conflicts of Interest

The authors declare that they have no conflicts of interest.

References

[1] M. H. Hussin and J. Kassim, "The corrosion inhibition and adsorption behavior of Uncaria gambir extract on mild steel in 1 M HCl," *Materials Chemistry and Physics*, vol. 125, pp. 461–468, 2010.

[2] H. J. Grahke, "Traité des Matériaux. Vol 12: Corrosion et chimie de surfaces des métaux. Von D. Landolt. Presses Polytechniques et Universitaires Romandes. Lausanne 1993. Preis: SF 118,–," *Materials and Corrosion*, vol. 45, pp. 146–146, 1994.

[3] O. K. Abiola, A. O. Aliyu, and S. Muhammed, "Anti-corrosive properties of Delonix regia extract on mild steel corrosion in acid fluid for industrial operations," *Science and Technology Journal*, vol. 2, no. 1B, pp. 489–491, 2017.

[4] M. H. Hussin, M. J. Kassim, N. Razali, N. Dahon, and D. Nasshorudin, "The effect of *Tinospora crispa* extracts as a natural mild steel corrosion inhibitor in 1 M HCl solution," *Arabian Journal of Chemistry*, vol. 9, pp. S616–S624, 2016.

[5] S. Şafak, B. Duran, A. Yurt, and G. Türkoğlu, "Schiff bases as corrosion inhibitor for aluminium in HCl solution," *Corrosion Science*, vol. 54, pp. 251–259, 2012.

[6] M. Abdallah, M. Sobhi, and H. Altass, "Corrosion inhibition of aluminum in hydrochloric acid by pyrazinamide derivatives," *Journal of Molecular Liquids*, vol. 223, pp. 1143–1150, 2016.

[7] X. Li, S. Deng, and X. Xie, "Experimental and theoretical study on corrosion inhibition of oxime compounds for aluminium in HCl solution," *Corrosion Science*, vol. 81, pp. 162–175, 2014.

[8] X. Li, S. Deng, and X. Xie, "Experimental and theoretical study on corrosion inhibition of *o* -phenanthroline for aluminum in HCl solution," *Journal of the Taiwan Institute of Chemical Engineers*, vol. 45, no. 4, pp. 1865–1875, 2014.

[9] I. Ahamad, R. Prasad, and M. Quraishi, "Adsorption and inhibitive properties of some new Mannich bases of Isatin derivatives on corrosion of mild steel in acidic media," *Corrosion Science*, vol. 52, no. 4, pp. 1472–1481, 2010.

[10] A. K. Singh and M. Quraishi, "Effect of Cefazolin on the corrosion of mild steel in HCl solution," *Corrosion Science*, vol. 52, no. 1, pp. 152–160, 2010.

[11] M. Abdallaha, O. Hazazia, A. Saada, S. El Shafeib, and A. Foudab, "Influence of N thiazolyl 2 cyanoacetamide derivatives on the corrosion of aluminum in 0.01 M sodium hydroxide1," *Protection of Metals and Physical Chemistry of Surfaces*, vol. 50, pp. 559–966, 2014.

[12] M. Abdallah, "Tetradecyl-1, 2-diol propenoxylates as inhibitors for corrosion of aluminium in hydrochloric acid," *Bulletin of Electrochemistry*, vol. 16, pp. 258–263, 2000.

[13] I. Obot, N. Obi-Egbedi, and S. Umoren, "The synergistic inhibitive effect and some quantum chemical parameters of 2,3-diaminonaphthalene and iodide ions on the hydrochloric acid corrosion of aluminium," *Corrosion Science*, vol. 51, no. 2, pp. 276–282, 2009.

[14] I. Issa, M. Moussa, and M. Ghandour, "A study on the effect of some carbonyl compounds on the corrosion of aluminium in hydrochloric acid solution," *Corrosion Science*, vol. 13, no. 10, pp. 791–797, 1973.

[15] G. Bereket and A. Yurt, "The inhibition effect of amino acids and hydroxy carboxylic acids on pitting corrosion of aluminum alloy 7075," *Corrosion Science*, vol. 43, no. 6, pp. 1179–1195, 2001.

[16] M. Lashgari and A. M. Malek, "Fundamental studies of aluminum corrosion in acidic and basic environments: theoretical predictions and experimental observations," *Electrochimica Acta*, vol. 55, no. 18, pp. 5253–5257, 2010.

[17] M. M. Fares, A. Maayta, and J. A. Al-Mustafa, "Corrosion inhibition of iota - carrageenan natural polymer on aluminum in presence of zwitterion mediator in HCl media," *Corrosion Science*, vol. 65, pp. 223–230, 2012.

[18] M. Desai, B. Thakar, P. Chhaya, and M. Gandhi, "Inhibition of corrosion of aluminium-51S in hydrochloric acid solutions," *Corrosion Science*, vol. 16, no. 1, pp. 9–24, 1976.

[19] H. El-Dahan, T. Soror, and R. El-Sherif, "Studies on the inhibition of aluminum dissolution by hexamine–halide blends: part I," *Weight Loss, Open Circuit Potential and Polarization Measurements, Materials Chemistry and Physics*, vol. 89, pp. 260–267, 2005.

[20] V. S. Saji, "A review on recent patents in corrosion inhibitors," *Recent Patents on Corrosion Science*, vol. 2, no. 1, pp. 6–12, 2010.

[21] M. Sangeetha, S. Rajendran, T. Muthumegala, and A. Krishnaveni, "Green corrosion inhibitors-an overview," *Zastita Materijala*, vol. 52, pp. 3–19, 2011.

[22] G. Broussard, O. Bramanti, and F. Marchese, "Occupational risk and toxicology evaluations of industrial water conditioning," *Occupational Medicine*, vol. 47, no. 6, pp. 337–340, 1997.

[23] P. B. Raja and M. G. Sethuraman, "Natural products as corrosion inhibitor for metals in corrosive media – a review," *Materials Letters*, vol. 62, no. 1, pp. 113–116, 2008.

[24] M. Znini, L. Majidi, A. Bouyanzer et al., "Essential oil of *Salvia aucheri mesatlantica* as a green inhibitor for the corrosion of steel in 0.5 M H_2SO_4," *Arabian Journal of Chemistry*, vol. 5, no. 4, pp. 467–474, 2012.

[25] S. Deng and X. Li, "Inhibition by *Jasminum nudiflorum* Lindl. leaves extract of the corrosion of aluminium in HCl solution," *Corrosion Science*, vol. 64, pp. 253–262, 2012.

[26] L. Bammou, M. Belkhaouda, R. Salghi et al., "Corrosion inhibition of steel in sulfuric acidic solution by the Chenopodium Ambrosioides extracts," *Journal of the Association of Arab Universities for Basic and Applied Sciences*, vol. 16, pp. 83–90, 2018.

[27] O. K. Abiola and Y. Tobun, "*Cocos nucifera* L. water as green corrosion inhibitor for acid corrosion of aluminium in HCl solution," *Chinese Chemical Letters*, vol. 21, no. 12, pp. 1449–1452, 2010.

[28] A. El-Etre, "Inhibition of acid corrosion of carbon steel using aqueous extract of olive leaves," *Journal of Colloid and Interface Science*, vol. 314, no. 2, pp. 578–583, 2007.

[29] P. C. Okafor, M. E. Ikpi, I. E. Uwah, E. E. Ebenso, U. J. Ekpe, and S. A. Umoren, "Inhibitory action of *Phyllanthus amarus* extracts on the corrosion of mild steel in acidic media," *Corrosion Science*, vol. 50, no. 8, pp. 2310–2317, 2008.

[30] H. K. Obied, M. S. Allen, D. R. Bedgood, P. D. Prenzler, K. Robards, and R. Stockmann, "Bioactivity and analysis of biophenols recovered from olive mill waste," *Journal of Agricultural and Food Chemistry*, vol. 53, no. 4, pp. 823–837, 2005.

[31] D. Bouknana, B. Hammouti, M. Messali, A. Aouniti, and M. Sbaa, "Phenolic and non-phenolic fractions of the olive oil mill wastewaters as corrosion inhibitor for steel in HCl medium," *Portugaliae Electrochimica Acta*, vol. 32, no. 1, pp. 1–19, 2014.

[32] M. Rguiti, M. Chadili, B. E. I. A. Baddouh, L. Bazzi, M. Hilali, and L. Bazzi, "Iron corrosion inhibition by olive mill wastewaters in acid medium," *Moroccan Journal of Chemistry*, vol. 6, p. 6-2, 2018, 307-317.

[33] I. B. Obot, K. Haruna, and T. A. Saleh, "Atomistic simulation: a unique and powerful computational tool for corrosion inhibition research," *Arabian Journal for Science and Engineering*, vol. 44, no. 1, pp. 1–32, 2019.

[34] B. el Ibrahimi, K. el Mouaden, A. Jmiai et al., "Understanding the influence of solution's pH on the corrosion of tin in saline solution containing functional amino acids using electrochemical techniques and molecular modeling," *Surfaces and Interfaces*, vol. 17, p. 100343, 2019.

[35] D. Bouknana, B. Hammouti, R. Salghi et al., "Physicochemical characterization of olive oil mill wastewaters in the eastern region of Morocco," *Journal of Materials and Environmental Science*, vol. 5, pp. 1039–1058, 2014.

[36] C. Verma, I. B. Obot, I. Bahadur, E.-S. M. Sherif, and E. E. Ebenso, "Choline based ionic liquids as sustainable corrosion inhibitors on mild steel surface in acidic medium: gravimetric, electrochemical, surface morphology, DFT and Monte Carlo simulation studies," *Applied Surface Science*, vol. 457, pp. 134–149, 2018.

[37] I. B. Obot, D. D. Macdonald, and Z. M. Gasem, "Density functional theory (DFT) as a powerful tool for designing new organic corrosion inhibitors. Part 1: an overview," *Corrosion Science*, vol. 99, pp. 1–30, 2015.

[38] S. John, A. Joseph, T. Sajini, and A. James Jose, "Corrosion inhibition properties of 1,2,4-hetrocyclic systems: electrochemical, theoretical and Monte Carlo simulation studies," *Egyptian Journal of Petroleum*, vol. 26, no. 3, pp. 721–732, 2017.

[39] M. Rguiti, A. Baddouh, K. Elmouaden, L. Bazzi, M. Hilali, and L. Bazzi, "Electrochemical oxidation of olive mill waste waters on tin oxide electrode," *Journal of Materials*, vol. 9, 558 pages, 2018.

[40] A.P.H. Association, A.W.W. Association, W. P. C. Federation, and W. E. Federation, *Standard Methods for the Examination of Water and Wastewater*, American Public Health Association, 1920.

[41] M. Rguiti, A. Baddouh, E. Amaterz et al., "Electrodegradation study of phenolic compounds containing in olive mill wastewaters of the chiadma region," *International Journal of Current Research*, vol. 10, pp. 67388–67395, 2018.

[42] N. Kovačević and A. Kokalj, "Analysis of molecular electronic structure of imidazole- and benzimidazole- based inhibitors: a simple recipe for qualitative estimation of chemical hardness," *Corrosion Science*, vol. 53, no. 3, pp. 909–921, 2011.

[43] M. S. Masoud, M. K. Awad, M. A. Shaker, and M. M. T. El-Tahawy, "The role of structural chemistry in the inhibitive performance of some aminopyrimidines on the corrosion of steel," *Corrosion Science*, vol. 52, no. 7, pp. 2387–2396, 2010.

[44] B. El Ibrahimi, A. Soumoue, A. Jmiai et al., "Computational study of some triazole derivatives (un- and protonated forms) and their copper complexes in corrosion inhibition process," *Journal of Molecular Structure*, vol. 1125, pp. 93–102, 2016.

[45] P. Dohare, K. R. Ansari, M. A. Quraishi, and I. B. Obot, "Pyranpyrazole derivatives as novel corrosion inhibitors for mild steel useful for industrial pickling process: experimental and quantum chemical study," *Journal of Industrial and Engineering Chemistry*, vol. 52, pp. 197–210, 2017.

[46] H. Bourzi, R. Oukhrib, B. El Ibrahimi et al., "Furfural analogs as sustainable corrosion inhibitors – predictive efficiency using DFT and Monte Carlo simulations on the Cu(111), Fe(110), Al(111) and Sn(111) surfaces in acid media," *Sustainability*, vol. 12, no. 8, p. 3304, 2020.

[47] A. Jmiai, B. El Ibrahimi, A. Tara, S. El Issami, O. Jbara, and L. Bazzi, "Alginate biopolymer as green corrosion inhibitor for copper in 1 M hydrochloric acid: experimental and theoretical approaches," *Journal of Molecular Structure*, vol. 1157, pp. 408–417, 2018.

[48] B. El Ibrahimi, A. Jmiai, K. El Mouaden et al., "Theoretical evaluation of some α-amino acids for corrosion inhibition of copper in acidic medium: DFT calculations, Monte Carlo simulations and QSPR studies," *Journal of King Saud University-Science*, vol. 32, no. 1, pp. 163–171, 2020.

[49] K. F. Khaled and M. M. al-Qahtani, "The inhibitive effect of some tetrazole derivatives towards Al corrosion in acid solution: chemical, electrochemical and theoretical studies," *Materials Chemistry and Physics*, vol. 113, no. 1, pp. 150–158, 2009.

[50] A. Jmiai, B. El Ibrahimi, A. Tara et al., "Application of *Zizyphus Lotuse* \- pulp of Jujube extract as green and promising corrosion inhibitor for copper in acidic medium," *Journal of Molecular Liquids*, vol. 268, pp. 102–113, 2018.

[51] M. M. Solomon and S. A. Umoren, "Electrochemical and gravimetric measurements of inhibition of aluminum corrosion by poly (methacrylic acid) in H_2SO_4 solution and synergistic effect of iodide ions," *Measurement*, vol. 76, pp. 104–116, 2015.

[52] I. V. Aoki, I. C. Guedes, and S. L. A. Maranhão, "Copper phthalocyanine as corrosion inhibitor for ASTM A606-4 steel in 16% hydrochloric acid," *Journal of Applied Electrochemistry*, vol. 32, no. 8, pp. 915–919, 2002.

[53] J. Bessone, C. Mayer, K. Jüttner, and W. Lorenz, "*AC* -impedance measurements on aluminium barrier type oxide films," *Electrochimica Acta*, vol. 28, no. 2, pp. 171–175, 1983.

[54] A. Esmail, H. Abed, M. Firdaous et al., "Physico-chemical and microbiological study of oil mill wastewater (OMW) from three different regions of Morocco (Ouazzane, Fes Boulman

and Béni Mellal)," *Journal of Materials and Environmental Science*, vol. 5, pp. 121–126, 2014.

[55] H. H. Hassan, E. Abdelghani, and M. A. Amin, "Inhibition of mild steel corrosion in hydrochloric acid solution by triazole derivatives: part I. Polarization and EIS studies," *Electrochimica Acta*, vol. 52, no. 22, pp. 6359–6366, 2007.

[56] A. Jmiai, B. El Ibrahimi, A. Tara et al., "Chitosan as an ecofriendly inhibitor for copper corrosion in acidic medium: protocol and characterization," *Cellulose*, vol. 24, no. 9, pp. 3843–3867, 2017.

[57] E. E. Oguzie, Y. Li, and F. H. Wang, "Effect of 2-amino-3-mercaptopropanoic acid (cysteine) on the corrosion behaviour of low carbon steel in sulphuric acid," *Electrochimica Acta*, vol. 53, no. 2, pp. 909–914, 2007.

[58] W. A. Badawy, K. M. Ismail, and A. M. Fathi, "Corrosion control of Cu-Ni alloys in neutral chloride solutions by amino acids," *Electrochimica Acta*, vol. 51, no. 20, pp. 4182–4189, 2006.

[59] C. Zou, X. Yan, Y. Qin, M. Wang, and Y. Liu, "Inhibiting evaluation of β-cyclodextrin-modified acrylamide polymer on alloy steel in sulfuric solution," *Corrosion Science*, vol. 85, pp. 445–454, 2014.

[60] H. Ashassi-Sorkhabi, B. Shabani, B. Aligholipour, and D. Seifzadeh, "The effect of some Schiff bases on the corrosion of aluminum in hydrochloric acid solution," *Applied Surface Science*, vol. 252, no. 12, pp. 4039–4047, 2006.

[61] S. Deng, X. Li, and H. Fu, "Two pyrazine derivatives as inhibitors of the cold rolled steel corrosion in hydrochloric acid solution," *Corrosion Science*, vol. 53, no. 2, pp. 822–828, 2011.

[62] A. Yurt, S. Ulutas, and H. Dal, "Electrochemical and theoretical investigation on the corrosion of aluminium in acidic solution containing some Schiff bases," *Applied Surface Science*, vol. 253, no. 2, pp. 919–925, 2006.

[63] Q. Zhang and Y. Hua, "Corrosion inhibition of aluminum in hydrochloric acid solution by alkylimidazolium ionic liquids," *Materials Chemistry and Physics*, vol. 119, no. 1-2, pp. 57–64, 2010.

[64] M. Lebrini, M. Lagrenée, H. Vezin, M. Traisnel, and F. Bentiss, "Experimental and theoretical study for corrosion inhibition of mild steel in normal hydrochloric acid solution by some new macrocyclic polyether compounds," *Corrosion Science*, vol. 49, no. 5, pp. 2254–2269, 2007.

[65] B. El Ibrahimi, A. Jmiai, A. Somoue, and R. Oukhrib, "Cysteine duality effect on the corrosion inhibition and acceleration of 3003 aluminium alloy in a 2% NaCl solution," *Portugaliae Electrochimica Acta*, vol. 36, no. 6, pp. 403–422, 2018.

[66] K. Krishnaveni and J. Ravichandran, "Effect of aqueous extract of leaves of Morinda tinctoria on corrosion inhibition of aluminium surface in HCl medium," *Transactions of Nonferrous Metals Society of China*, vol. 24, no. 8, pp. 2704–2712, 2014.

[67] E. A. Noor, "Evaluation of inhibitive action of some quaternary N-heterocyclic compounds on the corrosion of Al-Cu alloy in hydrochloric acid," *Materials Chemistry and Physics*, vol. 114, no. 2-3, pp. 533–541, 2009.

[68] M. A. Jingling, W. Jiuba, L. I. Gengxin, and X. V. Chunhua, "The corrosion behaviour of Al-Zn-In-Mg-Ti alloy in NaCl solution," *Corrosion Science*, vol. 52, no. 2, pp. 534–539, 2010.

[69] B. El Ibrahimi, A. Jmiai, K. El Mouaden et al., "Effect of solution's pH and molecular structure of three linear α-amino acids on the corrosion of tin in salt solution: a combined experimental and theoretical approach," *Journal of Molecular Structure*, vol. 1196, pp. 105–118, 2019.

[70] Y. Feng, S. Chen, W. Guo, Y. Zhang, and G. Liu, "Inhibition of iron corrosion by 5,10,15,20-tetraphenylporphyrin and 5,10,15,20-tetra-(4-chlorophenyl)porphyrin adlayers in 0.5 M H_2SO_4 solutions," *Journal of Electroanalytical Chemistry*, vol. 602, no. 1, pp. 115–122, 2007.

[71] L. Afia, R. Salghi, L. Bammou et al., "Anti-corrosive properties of argan oil on C38 steel in molar HCl solution," *Journal of Saudi Chemical Society*, vol. 18, no. 1, pp. 19–25, 2014.

[72] Y. Sangeetha, S. Meenakshi, and C. SairamSundaram, "Corrosion mitigation of *N*-(2-hydroxy-3-trimethyl ammonium)propyl chitosan chloride as inhibitor on mild steel," *International Journal of Biological Macromolecules*, vol. 72, pp. 1244–1249, 2015.

[73] A. Bousskri, A. Anejjar, M. Messali et al., "Corrosion inhibition of carbon steel in aggressive acidic media with 1-(2-(4-chlorophenyl)-2-oxoethyl)pyridazinium bromide," *Journal of Molecular Liquids*, vol. 211, pp. 1000–1008, 2015.

[74] P. Roy, A. Pal, and D. Sukul, "Origin of the synergistic effect between polysaccharide and thiourea towards adsorption and corrosion inhibition for mild steel in sulphuric acid," *RSC Advances*, vol. 4, no. 21, pp. 10607–10613, 2014.

[75] A. K. P. Chu and A. J. Sukava, "Cathode overpotential and electrosorption effects of straight-chain carboxylic acids during electrodeposition of copper," *Journal of the Electrochemical Society*, vol. 116, no. 9, pp. 1188–1193, 1969.

[76] Y. Sangeetha, S. Meenakshi, and C. Sairam Sundaram, "Corrosion inhibition of aminated hydroxyl ethyl cellulose on mild steel in acidic condition," *Carbohydrate Polymers*, vol. 150, pp. 13–20, 2016.

[77] H. Bhajiwala and R. Vashi, "Ethanolamine, diethanolamine and triethanolamine as corrosion inhibitors for zinc in binary acid mixture [HNO3+ H3PO4]," *Bulletin of Electrochemistry*, vol. 17, pp. 441–448, 2001.

[78] R. Menaka and S. Subhashini, "Chitosan Schiff base as ecofriendly inhibitor for mild steel corrosion in 1 M HCl," *Journal of Adhesion Science and Technology*, vol. 30, no. 15, pp. 1622–1640, 2016.

[79] M. A. Deyab, R. Essehli, and B. el Bali, "Inhibition of copper corrosion in cooling seawater under flowing conditions by novel pyrophosphate," *RSC Advances*, vol. 5, no. 79, pp. 64326–64334, 2015.

[80] M. Yadav, S. Kumar, R. R. Sinha, I. Bahadur, and E. E. Ebenso, "New pyrimidine derivatives as efficient organic inhibitors on mild steel corrosion in acidic medium: electrochemical, SEM, EDX, AFM and DFT studies," *Journal of Molecular Liquids*, vol. 211, pp. 135–145, 2015.

[81] N. Mora, E. Cano, J. L. Polo, J. M. Puente, and J. M. Bastidas, "Corrosion protection properties of cerium layers formed on tinplate," *Corrosion Science*, vol. 46, no. 3, pp. 563–578, 2004.

[82] M. P. Chakravarthy, K. N. Mohana, and C. B. Pradeep Kumar, "Corrosion inhibition effect and adsorption behaviour of nicotinamide derivatives on mild steel in hydrochloric acid solution," *International Journal of Industrial Chemistry*, vol. 5, no. 2, p. 19, 2014.

[83] S. S. A. el-rehim, S. A. M. Refaey, F. Taha, M. B. Saleh, and R. A. Ahmed, "Corrosion inhibition of mild steel in acidic medium using 2-amino thiophenoland 2-cyanomethyl benzothiazole," *Journal of Applied Electrochemistry*, vol. 31, no. 4, pp. 429–435, 2001.

[84] K. Fukui, "Role of frontier orbitals in chemical reactions," *Science*, vol. 218, no. 4574, pp. 747–754, 1982.

[85] D. Gustincic and A. Kokalj, "A DFT study of adsorption of imidazole, triazole, and tetrazole on oxidized copper surfaces: $Cu_2O(111)$ and $Cu_2O(111)$-w/o-Cu^{CUS}," *Physical Chemistry Chemical Physics*, vol. 17, no. 43, pp. 28602–28615, 2015.

[86] D. Gustincic and A. Kokalj, "DFT study of azole corrosion inhibitors on Cu_2O model of oxidized copper surfaces: I. Molecule–surface and Cl–surface bonding," *Metals*, vol. 8, no. 5, p. 310, 2018.

[87] M. K. Awad, M. S. Metwally, S. A. Soliman, A. A. el-Zomrawy, and M. A. bedair, "Experimental and quantum chemical studies of the effect of poly ethylene glycol as corrosion inhibitors of aluminum surface," *Journal of Industrial and Engineering Chemistry*, vol. 20, no. 3, pp. 796–808, 2014.

[88] M. K. Awad, M. R. Mustafa, and M. M. A. Elnga, "Computational simulation of the molecular structure of some triazoles as inhibitors for the corrosion of metal surface," *Journal of Molecular Structure: Theochem*, vol. 959, no. 1-3, pp. 66–74, 2010.

[89] S. Kaya, L. Guo, C. Kaya et al., "Quantum chemical and molecular dynamic simulation studies for the prediction of inhibition efficiencies of some piperidine derivatives on the corrosion of iron," *Journal of the Taiwan Institute of Chemical Engineers*, vol. 65, pp. 522–529, 2016.

[90] Y. Kharbach, F. Z. Qachchachi, A. Haoudi et al., "Anticorrosion performance of three newly synthesized isatin derivatives on carbon steel in hydrochloric acid pickling environment: electrochemical, surface and theoretical studies," *Journal of Molecular Liquids*, vol. 246, pp. 302–316, 2017.

[91] B. el Ibrahimi, L. Bazzi, and S. el Issami, "The role of pH in corrosion inhibition of tin using the proline amino acid: theoretical and experimental investigations," *RSC Advances*, vol. 10, no. 50, pp. 29696–29704, 2020.

[92] L. H. Madkour, S. Kaya, L. Guo, and C. Kaya, "Quantum chemical calculations, molecular dynamic (MD) simulations and experimental studies of using some azo dyes as corrosion inhibitors for iron. Part 2: Bis-azo dye derivatives," *Journal of Molecular Structure*, vol. 1163, pp. 397–417, 2018.

[93] B. El Ibrahimi, "Atomic-scale investigation onto the inhibition process of three 1,5-benzodiazepin-2-one derivatives against iron corrosion in acidic environment," *Colloid and Interface Science Communications*, vol. 37, article 100279, 2020.

[94] R. Oukhrib, B. El Ibrahimi, H. Abou Oualid et al., "In silico investigations of alginate biopolymer on the Fe (110), cu (111), Al (111) and Sn (001) surfaces in acidic media: quantum chemical and molecular mechanic calculations," *Journal of Molecular Liquids*, vol. 312, article 113479, 2020.